Picosecond excite-and-probe absorption measurement of the intra-$^2E_gE_{3/2}$-state vibrational relaxation time in $Ti^{3+}:Al_2O_3$

S. K. Gayen, W. B. Wang, V. Petričević, K. M. Yoo, and R. R. Alfano
Institute for Ultrafast Spectroscopy and Lasers, Physics Department and Electrical Engineering Department, The City College of New York, New York 10031

(Received 9 February 1987; accepted for publication 30 March 1987)

The kinetics of vibrational transitions in the $^2E_gE_{3/2}$ electronic state of $Ti^{3+}:Al_2O_3$ is studied by exciting higher lying vibrational levels of the state by a 527-nm picosecond pump pulse, and monitoring the subsequent growth of population in the zero vibrational level and lower lying vibrational levels by a 3.9-μm picosecond probe pulse. An upper limit of 3.5 ps for intra-$^2E_gE_{3/2}$-state vibrational relaxation time is estimated.

Recently, the trivalent titanium-ion-doped sapphire ($Ti^{3+}:Al_2O_3$) has been demonstrated[1] to be a tunable solid-state laser system with Ti^{3+} as the laser-active ion. A simple energy-level structure, broader tuning range, higher gain cross section, and the lack of any significant excited-state absorption (ESA) make $Ti^{3+}:Al_2O_3$ even a more promising tunable laser crystal than such chromium-based systems as alexandrite, GGG, and emerald. This potential has stimulated the recent interest in developing low-loss high-quality crystals of $Ti^{3+}:Al_2O_3$, and in investigating its spectroscopic and laser properties.[2–13] To our knowledge, there has been little effort to investigate the nonradiative relaxation processes and the kinetics of vibrational transitions in this crystal. Knowledge of these processes is crucial not only for understanding the physics behind tunable solid-state lasers, but also for characterizing new host materials for the Ti^{3+} ion. In this letter, we present the first picosecond time-resolved measurement of the relaxation kinetics among the vibrational levels of the lasing state in $Ti^{3+}:Al_2O_3$.

The single optically active $3d^1$ electron outside the closed argon core of Ti^{3+} determines the optical and spectroscopic properties of $Ti^{3+}:Al_2O_3$. The Ti^{3+} ion substitutes for octahedrally coordinated Al^{3+} in Al_2O_3 at sites with trigonal symmetry. As shown in Fig. 1(a) the cubic component of the crystal field (CF) splits the free-ion ^2D term of Ti^{3+} into a fourfold degenerate upper ^2E_g and a sixfold degenerate lower $^2T_{2g}$ manifold with an energy separation of 19 000 cm^{-1}.[12] These two manifolds are further split by the trigonal component of the CF, the spin-orbit interaction, and the dynamic Jahn–Teller (JT) interaction into five Kramer doublets.

The optical absorption spectrum of $Ti^{3+}:Al_2O_3$ is characterized by a double-humped absorption band spanning 400–600 nm, and is due to transitions from the ground $^2T_{2g}$ to the JT coupling-split $^2E_gE_{3/2}$ and $^2E_gE_{1/2}$ states. The broadband fluorescence spectrum covers the range 600–1050 nm at room temperature and originates in vibronic transitions from the $^2E_gE_{3/2}$ state to the states of the $^2T_{2g}$ manifold. The vibronic four-level mode of laser action in $Ti^{3+}:Al_2O_3$ at room temperature is tunable over the 660–986 nm continuous range of this fluorescence band. The absorption band in the blue-green region of the spectrum serves as the laser pump band. Because of the strong phonon coupling and the dynamic Jahn–Teller interaction, extremely rapid nonradiative relaxation follows resulting in population in the zero vibrational level (ZVL) and lower lying vibrational (LLV) levels of the $^2E_gE_{3/2}$ state.

The kinetic of these intra-$^2E_gE_{3/2}$ vibrational transitions has been investigated in our study. A 5-ps, 527-nm pulse excites a band of higher lying vibrational (HLV) levels of the $^2E_gE_{3/2}$ state and the subsequent growth of population in the ZVL and LLV levels is monitored by a 3.9-μm infrared probe pulse. Infrared transmission measurements are used to select this probe wavelength such that there is little ground-state probe absorption. The probe transition terminates on the HLV levels of the $^2E_gE_{3/2}$ and $^2E_gE_{1/2}$ states. The pump, probe, and relaxation transitions are shown schematically in the simplified configurational coordinate diagram in Fig. 1(b). The underlying assumption here is that the 3.9-μm probe pulse investigates the relaxed excited state population. Although the possibility of pumped HLV levels absorbing 3.9 μm photons and making transitions to still higher vibrational levels may not be completely ruled out, such transitions will terminate on the high-energy end of the $^2E_gE_{1/2}$ band. The Franck–Condon overlap integrals for such transitions are expected to be small, and hence contribution to 3.9-μm probe absorption due to such transitions may be neglected. Under this assumption, the kinetics of the vibrational transitions is studied by measuring the change in the induced absorption of the probe pulse as a function of the pump-probe delay time. Details of a similar experimental arrangement, detection scheme, signal averaging, and processing technique have been reported elsewhere.[14]

The Czochralski-grown $Ti^{3+}:Al_2O_3$ sample used in this experiment was obtained from the Electronics Division of Union Carbide Corp. The sample is a rectangular parallelepiped 22.5 mm × 10 mm × 9 mm in dimension and contains 0.12 at. % of Ti^{3+}. The induced absorption measurements were taken along the 9-mm path length of the sample. The radii of the pump and probe pulses at the sample position were 0.6 mm and 0.5 mm, respectively, and the pulses were made to cross the sample almost collinearly (a crossing angle of 2°).

The result of the present picosecond excite-and-probe measurement in $Ti^{3+}:Al_2O_3$ showing the time evolution of the optical density (OD) at 3.9 μm in the excited $^2E_gE_{3/2}$ state at room temperature is shown in Fig. 2. The curve is characterized by a sharp rise followed by a long decay. The

 0003-6951/87/211494-03$01.00

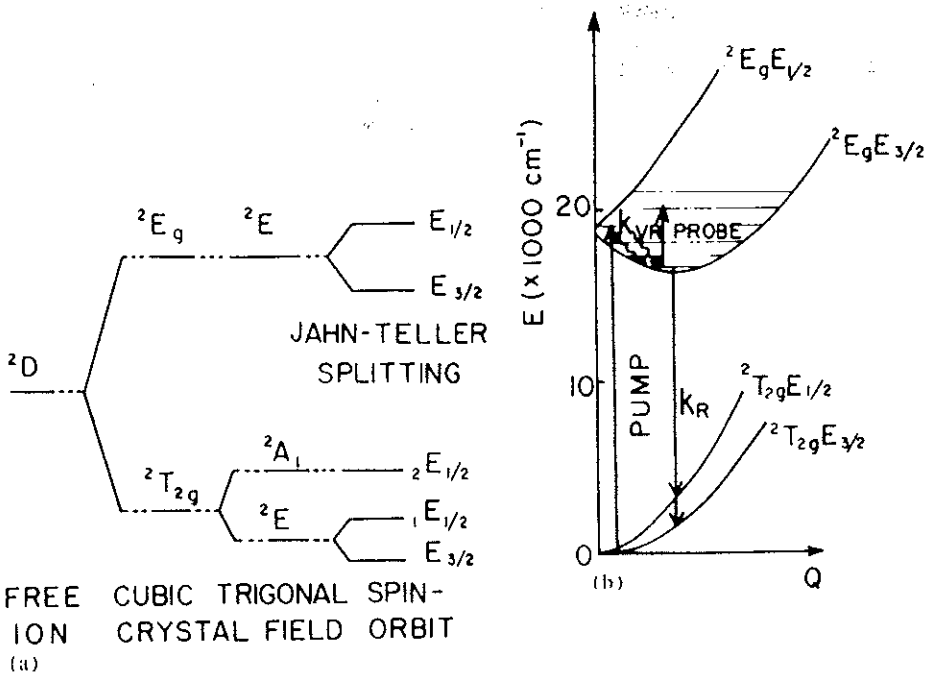

FIG. 1. (a) Energy-level diagram of Ti^{3+}:Al_2O_3 showing the splitting of the ^2D term by the cubic and trigonal crystal fields, the spin-orbit coupling, and the dynamic Jahn–Teller interaction. (b) Corresponding simplified configurational coordinate diagram showing the pump, probe, and relaxation transitions.

long lifetime decay reflects the depopulation of the zero and lower lying vibrational levels of the $^2E_gE_{1/2}$ state via radiative transitions. Since the room-temperature fluorescence lifetime is 3.15 ± 0.5 μs[7] there is no appreciable change in the population over the time scale of this measurement.

The rise time (time for growth of OD from 10 to 90 %) is ~ 9 ps. In order to account for the group dispersion effects, the transit times for both the 527-nm pump pulse and the 3.9-μm probe pulse through the 9-mm sample path were calculated using the dispersion characteristics of sapphire.[15] The two transit times differ by 1.5 ps, which is the upper limit for uncertainty in the rise time from group dispersion effects. In order to extract a value for the vibrational relaxation time, we use a rate-equation analysis of the experimental data. The rate equations governing the population kinetics in the $^2E_gE_{1/2}$ state are

$$\frac{dN_2}{dt} = -k_{VR}N_2 + \alpha LP(t)\,, \tag{1}$$

$$\frac{dN_1}{dt} = k_{VR}N_2 - k_RN_1\,, \tag{2}$$

where $N_1(t)$ is the instantaneous population density in the ZVL and LLV levels and $N_2(t)$ is the instantaneous population density in the pumped HLV levels of the $^2E_gE_{1/2}$ state, k_{VR} and k_R are the vibrational and radiative relaxation rates, $P(t)$ is the pump-photon flux density, α is the ground-state absorption coefficient for the pump pulse, and L is the length of the sample. Equation (1) assumes $\alpha L \ll 1$. The rate equations were solved numerically using the fourth-order Runge–Kutta method,[16] and the profile of the pump pulse was taken as a Gaussian[17] of 5-ps FWHM.

The measured change in the optical absorption of the probe pulse at a particular delay time t_d is given in terms of $N_1(t)$ by

$$\mathrm{OD}(t_d) = -\ln\left[\int I(t-t_d)\exp[-\sigma_e L N_1(t)]\,dt \Big/ \int I(t)\,dt\right], \tag{3}$$

where $I(t)$ is the intensity and σ_e is the excited state absorption cross section of the probe pulse, respectively. A fit of the experimental data to Eq. (3) assuming a Gaussian probe pulse[18] of estimated 3.5 ± 0.5 ps FWHM and using k_{VR} as a variable parameter is displayed in Fig. 2. The excited state absorption cross section σ_e is estimated from the measured optical density at much larger delay times (flat region of the curve) to be $\sim 4 \times 10^{-18}$ cm^2.

The best fit to the experimental data yields a value of 2.0 ± 1.5 ps for the intra-$^2E_gE_{1/2}$-state vibrational relaxation time k_{VR}^{-1} in Ti^{3+}:Al_2O_3. However, k_{VR}^{-1} is less than 3.5 ps even at the extreme limit of the experimental signal-to-noise ratio. Since the observed system response is smaller than the widths of the pump and probe pulses, its precise determination depends strongly on the accurate knowledge of the duration of those pulses. The estimated group dispersion effect, though small, would cause a broadening of the rising edge of the probe absorption curve. Since all these factors contribute to an overestimation of the system response, we take 3.5 ps to be an upper limit for the intra-$^2E_gE_{1/2}$-state vibrational relaxation time in Ti^{3+}:Al_2O_3. This time is much shorter than 17 ps obtained for the intra-$^4T_2$ vibrational relaxation time in alexandrite,[19] but may be comparable to vibrational relaxation times in organic molecules like fluorescein, naphthalene, parabenzoquinone, rhodamine dyes, etc.[20]

Since there is a single phonon of energy 173 cm^{-1} that interacts with the excited ^2E_g state[6,13] of Ti^{3+}:Al_2O_3, a rough estimate of the "effective phonon emission time" in the ^2E_g state of this system may be made. The energy degra-

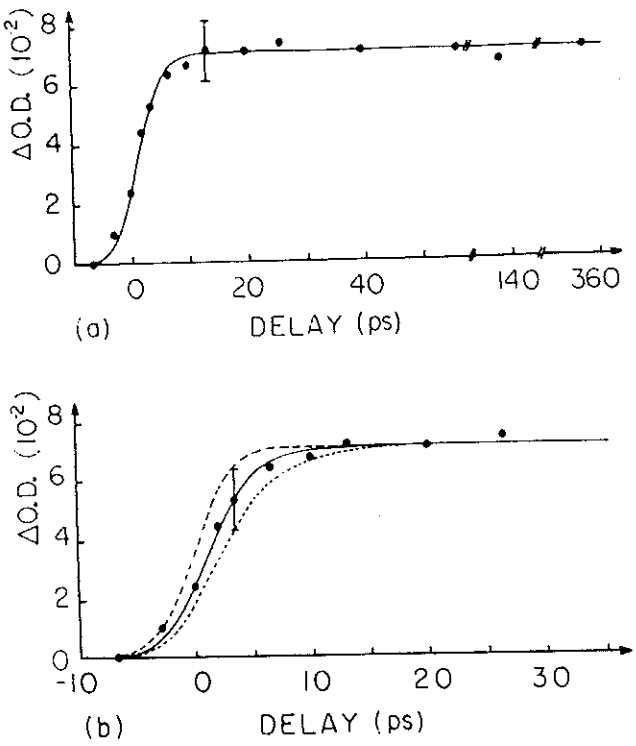

FIG. 2. (a) Time evolution of the optical density at 3.9 μm in the zero vibrational level and the lower lying vibrational levels in $Ti^{3+}:Al_2O_3$ at room temperature. The zero time is accurate within 5 ps. The size of a typical error bar is shown. The closed circles represent the experimental measurements and the solid curve is a computer fit to the data using the rate equations and a relaxation time k_{1R}^{-1} of 2 ps. (b) The rising portion is shown on an expanded scale along with fits corresponding to relaxation times of 0.5, 2, and 3.5 ps. It is evident that the relaxation time k_{1R}^{-1} is less than 3.5 ps.

dation process from the pumped HLV levels to the zero vibrational level involves emission of 15 phonons. Assuming that the vibrational relaxation process is serial in this system, the effective phonon emission time will be $\leqslant$ 230 fs, 1/15 of the estimated vibrational relaxation time. This time is consistent with the electron-phonon scattering time of 165 fs in GaAs.[21] However, the details of the relaxation mechanism of excited impurity ions in insulators are presumably different from those of optically excited carriers in polar semiconductors. A detailed understanding of these mechanisms presents an interesting problem for further theoretical and experimental investigations.

We gratefully acknowledge Dr. M. Kokta of Union Carbide Corp. for providing us with the crystals used in this measurement and Dr. C. Byvik of National Aeronautics and Space Administration for earlier samples. The research is supported by Army Research Office and National Aeronautics and Space Administration.

[1] P. F. Moulton, Opt. News **8**, 9 (1982); Opt. Lett. **10**, 273 (1985).
[2] B. K. Sevast'yanov, Kh. S. Bagdasarov, E. A. Federov, V. B. Semenov, I. N. Tsigler, K. P. Chirkina, L. S. Starostina, A. P. Chirkin, A. A. Minaev, V. P. Orekhova, V. P. Seregin, A. N. Kolerov, and A. N. Vratskii, Sov. Phys. Crystallog. **29**, 566 (1984).
[3] G. F. Albrecht, J. M. Eggleston, and J. J. Ewing, Opt. Commun. **52**, 401 (1985).
[4] R. C. Powell, J. L. Caslavsky, Z. AlShaieb, and J. M. Bower, J. Appl. Phys. **58**, 2331 (1985).
[5] P. Lacovara, L. Esterowitz, and M. Kokta, IEEE J. Quantum Electron. **QE-21**, 1614 (1985).
[6] C. E. Byvik and A. M. Buoncristiani, IEEE J. Quantum Electron. **QE-21**, 1619 (1985).
[7] P. F. Moulton, J. Opt. Soc. Am. B **3**, 125 (1986) and Ref. 1 therein.
[8] P. Albers, E. Stark, and G. Huber, J. Opt. Soc. Am. B **3**, 134 (1986).
[9] E. D. Nelson, J. Y. Wong, and A. L. Schawlow, Phys. Rev. **156**, 298 (1967).
[10] R. R. Joyce and P. L. Richards, Phys. Rev. **179**, 375 (1968).
[11] R. M. Macfarlane, J. Y. Wong, and M. D. Sturge, Phys. Rev. **166**, 250 (1968).
[12] D. S. McClure, J. Chem. Phys. **36**, 2757 (1962).
[13] B. F. Gächter and J. A. Koningstein, J. Chem. Phys. **60**, 2003 (1974).
[14] S. K. Gayen, W. B. Wang, V. Petričević, R. Dorsinville, and R. R. Alfano, Appl. Phys. Lett. **47**, 455 (1985).
[15] Irving H. Maltison, J. Opt. Soc. Am. **52**, 1377 (1962).
[16] Michael J. Romanelli, in *Mathematical Methods for Digital Computers*, edited by A. Ralston and H. S. Wilf (Wiley, New York, 1960), p. 110.
[17] N. H. Schiller, M. Foresti, and R. R. Alfano, J. Opt. Soc. Am. B **2**, 729 (1985).
[18] A. Seilmeier, K. Spanner, A. Laubereau, and W. Kaiser, Opt. Commun. **24**, 237 (1978).
[19] S. K. Gayen, W. B. Wang, V. Petričević, and R. R. Alfano, Appl. Phys. Lett. **49**, 437 (1986).
[20] R. Englman, *Nonradiative Decay of Ions and Molecules in Solids* (North-Holland, Amsterdam, 1979), p. 281.
[21] J. A. Kash, J. C. Tsang, and J. M. Hvam, Phys. Rev. Lett. **54**, 2151 (1985).